Influence of Impeller Type on Hydrodynamics and Gas-Liquid Mass-Transfer in Stirred Airlift Bioreactor

Sérgio S. de Jesus, João Moreira Neto, Aline Santana, and Rubens Maciel Filho
Laboratory of Optimization, Design and Advanced Control, School of Chemical Engineering, University of Campinas, CEP 13083-852, Campinas, SP, Brazil

DOI 10.1002/aic.14871
Published online May 25, 2015 in Wiley Online Library (wileyonlinelibrary.com)

The influence of impeller type in a mechanically stirred airlift bioreactor was analyzed in relation to the non-Newtonian viscous fluids. The agitation was carried out through a marine impeller (axial impeller) and a paddle impeller (radial impeller) located along with the gas sparger in the region comprised by the riser. The bioreactor was sparged with air under different velocities (0.036–0.060 m s^{-1}). Carboxymethylcellulose 1.94% and xanthan 1.80% were used as a fluid model. The gas holdup and volumetric mass-transfer coefficient increased in up to five and three times, respectively, when compared to a conventional airlift bioreactor; however, better results were obtained when the straight paddle impeller type was used. The results suggest that the studied bioreactor can be used successfully in viscous fluid, and it can be more efficient than conventional airlift bioreactors. The results obtained suggest the use of radial impellers.
 AIChE J, 61: 3159–3171, 2015
Keywords: agitation, airlift bioreactor, hydrodynamics, impeller, mass transfer, non-Newtonian fluids

Introduction

The influence of viscosity in the oxygen transfer occurring in fermentation broths with non-Newtonian behavior presents a considerable challenge in the attainment of an efficient aeration and agitation system.[1–4] Unfortunately, high aeration and agitation can cause increased foaming, which in turn causes the loss of volatile metabolites and the shear rate increase, causing cellular damage often resulting in the reduction of cell growth, and consequently the process yield.[5] The use of airlift bioreactors in highly viscous and non-Newtonian processes demonstrated lower shear rate in relation to the mechanically stirred bioreactor. However, the volumetric mass-transfer coefficient decreases with the increasing viscosity of the medium. The effective interfacial area and the low homogenization of the cell culture decrease because of the high viscosity that the medium produces, which may be insufficient when used at a preindustrial or industrial scale. The low mixing efficiency also limits the homogenization of the medium and the oxygen transfer.[6–11] In industry, the stirred tank reactor is often preferred for aerobic fermentation when high oxygen transfer rates are required. The airlift reactor is rather found in water treatment plants as it offers good mixing and acceptable oxygen transfer rates at low operating cost. Many studies in the literature have attempted to mix these two concepts (stirred and airlift reactors). However, experimental results in this type of devices are difficult to analyze accurately as many hydrodynamic parameters are closely linked. This explains why some studies lead to different interpretation. Pioneer studies conducted by Pollard et al.,[7] Chisti and Jauregui-Haza[8] with non-Newtonian fluids in hybrid bioreactors showed that the agitation significantly increases the gas holdup and the volumetric oxygen transfer coefficient. Nonetheless, they were unable to verify the influence of agitation on the shear rate. The proper choice of the impeller type used in highly viscous and non-Newtonian fluids have been described in the literature[12–14]; however, there are no studies regarding the proper choice of an impeller to be used in non-Newtonian and highly viscous fluids in a mechanically stirred airlift bioreactors.

The performance of stirred airlift bioreactors has been studied mainly in terms of volumetric oxygen transfer coefficient. The effects of the impeller type on the hydrodynamics and gas-liquid mass transfer in stirred airlift bioreactors need to be studied. The impact of the impeller type may be directly related to the process efficiency and output. Studies that show the performance of these bioreactors in viscous fluid and the influence of the impeller type in the efficiency of this equipment have been scarce.

The scope of this study is to contribute, through experimental data, with some aspects of hydrodynamics and oxygen transfer yet unexplored in studies of hybrid airlift bioreactors when agitated with radial or axial impellers. Through the results obtained and discussed in this article, we hope to contribute to a better understanding of these types of bioreactors, and through the data published in this article we hope it will contribute to studies of scale up.

The specific objective of this work was to study, through comparative analysis, the influence of a radial impeller and an axial impeller agitation on an airlift bioreactor of internal recirculation and concentric tubes; the stirring system was promoted by the impeller located at the end of the gas sparger, in the area comprised by the riser. In this study, we used two

Correspondence concerning this article should be addressed to S. S. de Jesus at ssjesus@gmail.com.

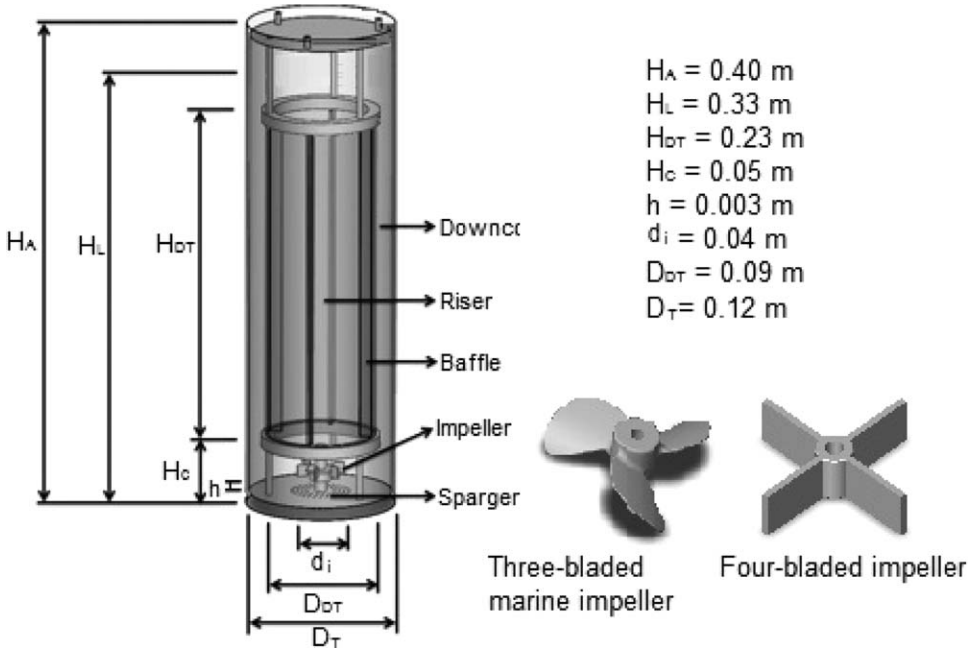

Figure 1. The schematic diagram of the experimental bioreactor system.

types of impellers, one of them is an axial three-blade marine impeller, and the other one is a radial four-blade paddle impeller with the same diameter and using non-Newtonian viscous fluids, which we evaluated in relation to hydrodynamics and oxygen transfer.

Experimental Section

Bioreactor and fluids

We performed the experiments in a concentric draft-tube stirred airlift bioreactor. The stirring systems are located on the lower part of the bioreactor, in the middle of the gas sparger plate, and in the area comprised by the riser to increase the bursting of the bubbles. During the experiments there were observed three types of flow behavior, at low gas velocities (0.0157 m s^{-1}) bubbles stagnated in the riser. Increasing the speed, caused a stagnation of bubbles in the downcomer, high gas velocities caused a complete recirculation of the riser bubbles to the downcomer.

To prevent a vortex from being created, four baffles were introduced inside the inner tube, in the riser. The air was sparged into the internal zone through a circular perforated plate with 0.05 m of diameter, containing 90 equidistant holes measuring 0.001 and 0.003 m, located at the bottom of the bioreactor, concentric in relation to the area comprised by the riser. The work volume of the bioreactor was 3.5 L. Dimensions are shown in Figure 1. A dissolved oxygen electrode (O2-sensor InPro6800/12/220 Mettler Toledo, Switzerland) was positioned at the centerline of the vessel and 0.15 m above the bottom of the tank. Two identical pH probes (405-DPAS-SC-K8S/225 Mettler Toledo, Switzerland) was used. The vertical distance between the pH probes was 0.10 m; the lower probe was 0.10 m above the base of the tank and directly below the upper pH probe.

The reactor was sparged with oxygen or nitrogen. Carboxymethylcellulose solutions (CMC) 1.94% (MP Biomedicals, France, PM 262.19 g mol^{-1}) and xanthan gum 1.80% prepared with deionized water (Sigma-Aldrich, PM 4.2×10^6 Da) were used as non-Newtonian fluid models. The superficial oxygen velocity in the riser (U_{GR}) ranged from 0.0157 to 0.0262 m s^{-1}. An axial three-bladed marine impeller or a radial four-bladed paddle impeller with the same geometric similarities and 40 mm of diameter (Figure 1) made stirring. The stirring speed ranged from 0 to 800 rpm. All experimental runs were carried out at atmospheric pressure and a temperature of 25°C.

The measurements

Rheology. The rheological behaviors of the fluids used in this study were correlated with two models described in the literature. The apparent viscosity (μ_{ap}) was estimated according to the power law (Ostwald–de Wale), given by

$$\mu_{ap} = k\gamma_m^{n-1} \tag{1}$$

where γ_m is the average shear rate, k and n are experimental parameters of the model.

The yield stress produced by the fluid, was obtained using an approximation of the rheological behavior of non-Newtonian fluids, which in the Herschel and Bulkley model, was used and given by

$$\tau = \tau_0 + k'\dot{\gamma}^{n'} \tag{2}$$

where τ is the shear stress, τ_0 is the yield stress, k' and n' are experimental parameters of the model.

The analysis of k, k', n, and n' parameters were determined using a coaxial cylinders ZA-30 (coquette) HAAKE RheoStress 6000 rheometer (Thermo Scientific, Victoria, Australia), with 60 mm in diameter.

The density (ρ) and superficial tension of the solutions (σ) were measured by the force tensiometer model K20 (Krüs, Hamburg, Germany).

Mixing Time. The mixing time was determined by the acid tracer technique,[15,16] as the time needed for the tracer concentration to reach 95% of its final steady-state value from the moment of tracer input. Once the reactor was filled with the corresponding fluid, HCl (35% wt/vol) was added up to pH

2, and the air was bubbled for 20 min ($UG = 0.030$ m s^{-1}) to remove any carbonate. Then, with NaOH (6 M), the pH was established at 5.50 ± 0.05. The acid tracer (1 mL of HCl 35% wt/vol) was added in the reactor through a port in the riser section. All experiments were carried out in triplicate.

The dimensionless concentration C_T of the tracer (hydrogen ion) was calculated as follows

$$C_T = \frac{[H^+]_{instantaneous} - [H^+]_{initial}}{[H^+]_{final} - [H^+]_{initial}} \quad (3)$$

Gas Holdup. The total gas holdup (ε_G) was measured by the volume expansion method, as follows[15]

$$\varepsilon_G = \frac{h_D - h_L}{h_D} \quad (4)$$

where h_D is the height of gas-liquid dispersion and h_L is the height of gas free liquid.

Volumetric Oxygen Transfer Coefficient. The overall gas-liquid volumetric mass transfer coefficient (k_La) was measured with the dynamic gassing-in method.[17] For each test, the fluid was purged by bubbling nitrogen until it reached a dissolved oxygen concentration lower than 5% of air saturation. Then, the nitrogen flow was suspended, the bubbles were released, and the airflow was established according to the required conditions. The increase in the dissolved oxygen concentration was followed with time until the fluid became nearly saturated with oxygen (>90%); k_La was calculated as the slope of the linear equation

$$-\ln(1-E) = k_La(t - t_0) \quad (5)$$

where E is the fractional approach to equilibrium and can be estimated by[15]

$$E = \frac{C - C_0}{C^* - C} \quad (6)$$

where C^* is the dissolved oxygen saturation concentration, C_0 is the dissolved oxygen initial concentration at t_0 time when a hydrodynamic steady state has been reestablished ($\leq$60 s) upon the beginning of aeration, and C is the dissolved oxygen concentration at any t time.

Power Measurement. The power input due to mechanical stirring was calculated using the power number (N_P).

The power number for each impeller and in the studied fluids was determined experimentally.

The torque was determined by an optical-electronic measuring device (Dataflex 22/50, KTR, Germany).

The power number for each impeller was calculated using the equation given by

$$N_P = \frac{P_0}{\rho_L N^3 d_i^5} \quad (7)$$

where P_0 is the power drawn under ungassed conditions, and N is the stirring speed. The power is related is related to the imposed torque (M) on the rotating shaft, by the relationship[6]

$$P_0 = 2\pi\ N\ (M - M_0) \quad (8)$$

where M_0 is subtracted to account for power losses in the motor, gearbox, bearings, and seals.

Usually, in the turbulent regime the power number is found to be a constant and is specific to the type of impeller and the geometry of the impeller. In laminar or transitional flow regime, however, it is inversely proportional to the Reynolds number.[18]

In non-Newtonian fluids, the viscosity is a function of shear rate, therefore, the expression for Re has been modified in accordance with the fluid rheology.

In this study, we adopted the Rieger and Novak method, which consists of measuring the effective viscosity of the fluid at a shear rate equal to the rate of rotation.

Using the power law viscosity model, this yields[19]

$$Re = \frac{\rho N^{2-n} d_i^2}{k} \quad (9)$$

Bubble Size. The average bubbles size was measured photographically according Fadavi et al.[20] The images were taken from the outer wall of the reactor near the gas sparger, in the middle and top of the bioreactor (end of the liquid) column. To minimize distortion of the generated images, a minimum of 200 images of bubbles were taken for each hydrodynamic steady state. Lengths of the major and minor axes of the projected images of ellipsoidal bubbles were measured using the software AUTOCAD® 2012. The diameter d_B of the volume-equivalent sphere for the ellipsoidal bubble was calculated as follows[20]

$$d_B = (x \cdot y^2)^{1/3} \quad (10)$$

where x and y are the lengths of the major and minor axes of the ellipsoid in the two-dimensional projection, respectively

The error was calculated by

$$\varepsilon = \frac{s}{\sqrt{m}} \quad (11)$$

where ε is the error, s is the standard deviation is defined as the square root of the average squared difference from the mean ($s = \sqrt{\frac{1}{m-1}\sum_{i=1}^{n}(d_{Bi} - \overline{d_B})}$ and $\overline{d_B} = \frac{1}{m}\sum_{i=1}^{n} d_{Bi} = \frac{d_{B1} + d_{B2} + \ldots + d_{Bm}}{m}$), m stands for the size of the sample.

Results and Discussions

Table 1 presents the physical constants used for the calculations. Figure 2 presents the rheological characterization of the fluids.

Mixing time

The mixing times as a function of the superficial gas velocity for both types of impellers used in our studies and under different stirring speeds are presented in Figure 3. Mixing time decreased linearly with the superficial gas velocity. Studies conducted in stirred bioreactors showed that mixing in the bioreactor is caused by the action of the impeller, aeration, or by the action of both.[24] The experiments performed for both fluids showed that low rotational speeds help to reduce the mixing time; however, we observed that in rotations above 400 rpm there was a small increase in mixing time. According to Nienow[25] with high speed stirring, the impeller is unable to disperse gas, that is, the impeller is flooded, and aeration improves mixing due to the action of the plume of air bubbles. This effect was observed when employing the axial and radial impeller, in which case the higher speeds of rotation and aeration presented the adhesion of bubbles to the impeller. The higher rotation causes the liquid to be directed to the base or to the bottom wall of the reactor; therefore, failing to generate sufficient turbulence for the proper circulation of the liquid. These observations have a major impact on the process variables, since to obtain a higher rotation speed, greater mechanical power is needed in order to move the impeller, which leads

Table 1. Properties of Liquids Used

Fluid	Temperature (°C)	ρ (Kg m^{-3})	τ_0 (Pa)	n	k (Pa s^n)	n'	k' (Pa s^n)	$\sigma \times 10^3$ (Nm^{-1})	$D_L \times 10^9$ (m^2 s^{-1})
CMC 1.94%	25	1005[c]	7.77[c]	0.34[c]	0.68[c]	0.33[c]	8.31[c]	67.20[c]	2.03[a]
Xanthan 1.80%	25	1001[c]	11.23[c]	0.21[c]	0.87[c]	0.22[c]	13.70[c]	51.00[c]	0.31[b]

[a]Retired from Godbole et al.[21]; Linek and Sinkule.[22]
[b]Retired from Terasaka and Shibata.[23]
[c]Experimental dates.
n and k obtained by the Ostwald–de Wale model.
n' and k' obtained by the Herschel and Bulkley model.

to greater power consumption, in addition to an increase in shear rate, and mixing time.

Gas holdup

Figure 4 shows the gas holdup from the CMC/air and xanthan/air systems depending on the superficial gas velocity at different speeds of rotation. The agitation increased the gas fraction in the bioreactor, and this increase was greater with a paddle impeller, in the order of up to four times when CMC was used as model fluid; with the xanthan gum solution, the agitation favored the holdup up to five times higher than the obtained without agitation (Figures 4a, b). However, the gas fraction was very low, especially when using xanthan gum as model fluid. The increased viscosity is a critical factor that must be taken into consideration when choosing the bioreactor. Non-Newtonian viscous fluids generally have low gas holdup, independently of the reactor type. The lower the n index of the Ostwald–de Waele model (Eq. 1; Table 1), the higher is the apparent viscosity, in other words, the gas holdup values decrease with an increase in degree of pseudoplasticity. The increase in the gas holdup fraction from the bioreactor column is directly related to the increase of the aeration and agitation imposed, the formation of small bubbles caused by

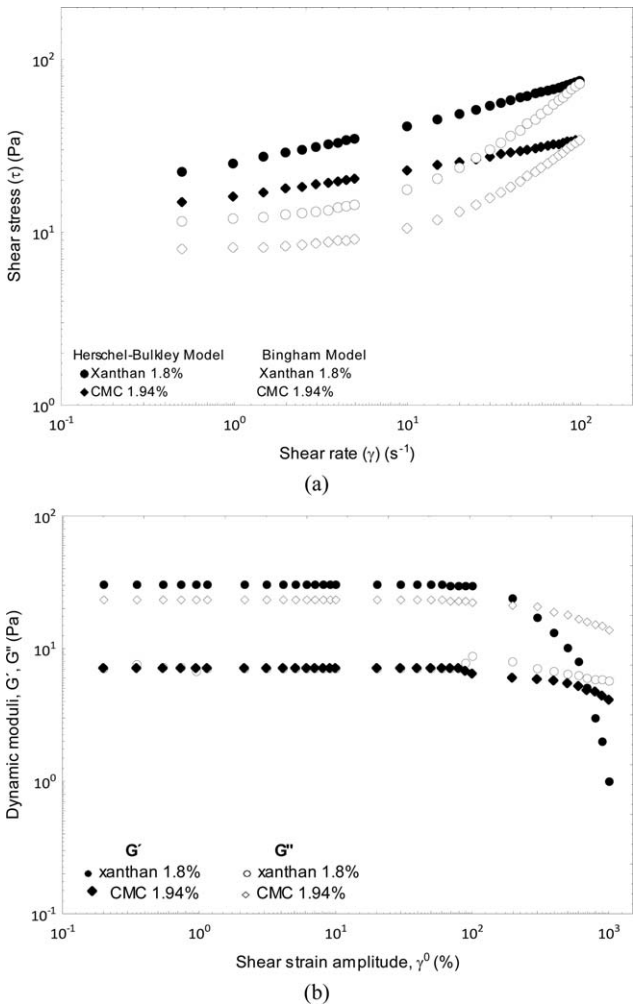

Figure 2. Rheological behavior of the liquids used. (a) Bingham and Herschel–Bulkley model. (b) The dependence of storage modulus, G', and loss modulus G'', on shear strain amplitude, γ^0.

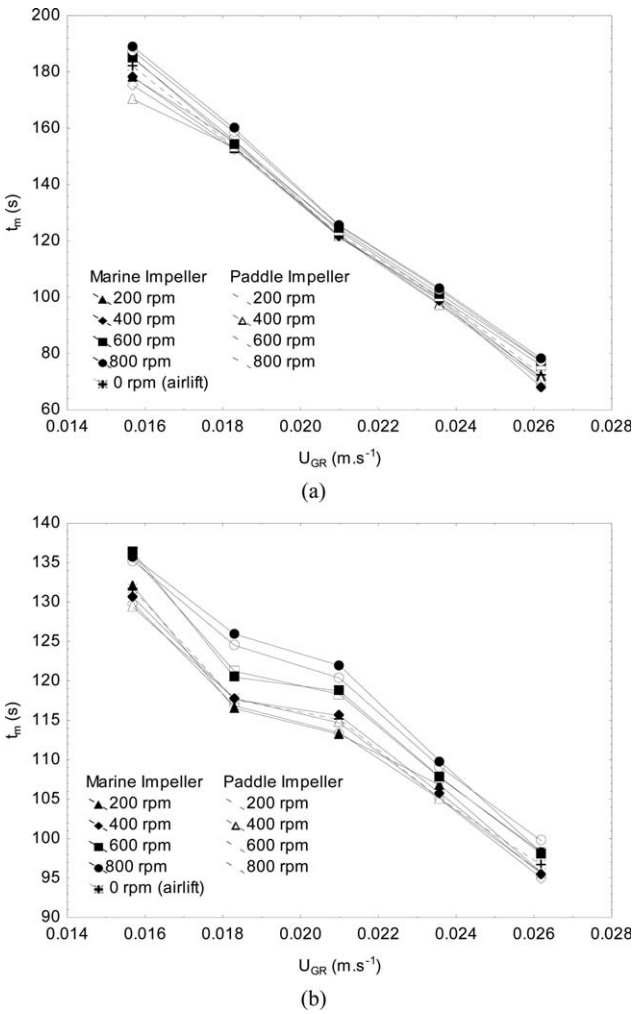

Figure 3. Effect of the impeller agitation speed and the aeration velocity on the mixing time for CMC 1.94% (a) and xanthan 1.80% (b).

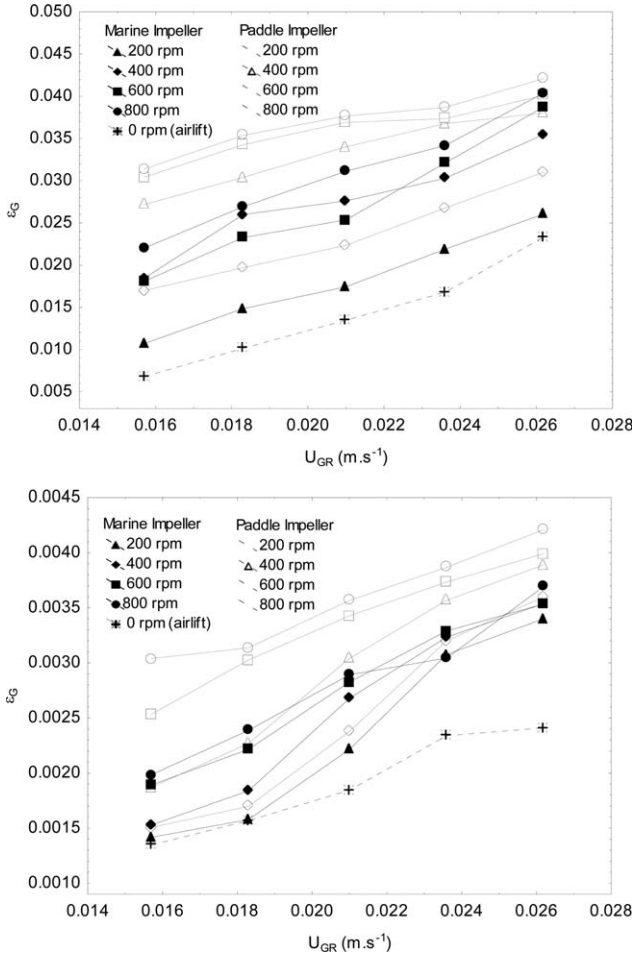

Figure 4. Effect of impeller agitation speed and the aeration velocity on the overall gas holdup for for CMC 1.94% (a) and xanthan 1.80% (b).

aeration/agitation are usually generated by the following mechanisms[26]: (1) during the coalescence process between the bubbles near the gas distributor plate, the trailing big bubble elongates causing its tail break up into small bubbles; (2) a large bubble breaking up at the surface of the liquid generates small bubbles; (3) small bubbles can be obtained by the creation of sufficient turbulence in the liquid to break up larger bubbles. This phenomenon also occurs when the gas flow rate is high; thus, causing a strong liquid circulation. With the xanthan gum experiments, there was an upsurge in the formation of small bubbles triggered by the increase in aeration, this is probably due to the fact that xanthan is active as a surfactant; thus, partially contributing to the increased gas holdup. Conversely, with the CMC there were no small bubbles; however, we observed that some of the bubbles coalesced primarily in the center of the riser, most likely a result of the agitation and the characteristics of the fluid. We can see in Table 1 that the fluid surface tensions decreased with the reduction of the n index of the power law model (Eq. 1).

We believe that the results demonstrate that airlift bioreactors with mechanical stirring may be used in mediums, which exhibit non-Newtonian behavior and highly viscous. Experiments with CMC have also shown that a significant fraction of gas was retained in the bioreactor (Figure 4a); this retention is probably related to the fluid movement from the riser to the downcomer, aided mainly by the action of the impeller, which contributed, in part, for the bubbles to break up into smaller ones. Conversely, we also observed the formation of coalescing bubbles due to the partial restriction of bubbles movement caused by the high viscosity of the fluid, resulting in the decrease in the ascending rate of these bubbles, causing greater number of collisions between them, thus leading to their coalescence; these coalescing bubbles also contributed to the increase in gas holdup.[26]

Studies with xanthan gum showed that small bubbles could not escape from the liquid by their buoyancy due to the yield stress of the liquid. Our studies with xanthan gum verified that at first the agitation favored the breaking and formation of small bubbles; however, these have stagnated mainly in the downcomer region because the agitation was not strong enough to cause their displacement at a given speed of rotation. We believe that the agitation favored the flinging of these bubbles against the wall of the reactor, mainly in the lower downcomer; moreover, fluid displacement from the riser to the downcomer caused by aeration also contributed for the bubbles stagnation in the middle of the column in the downcomer region; thus, preventing the formation of a riser-downcomer cycle. Terasaka and Shibata,[23] observed that, in xanthan aqueous solutions, the yield stress caused the accumulation of very small bubbles. Table 1 and Figure 2 show that the xanthan solution also presents yield stress. This could also confirm the accumulation of small bubbles on the wall of the bioreactor. According to Kawalec-Pietrenko,[26] the small bubbles relative contribution increases with the increase in the liquid viscosity; therefore, confirming our observations. In the center of the reactor, the region encompassed by the riser, there was the formation of coalescing bubbles caused primarily by the increased collision among the bubbles in this region, which is located in the gas sparger. Studies using xanthan solutions in airlift bioreactors demonstrated that large bubbles produced faster bubble rise velocities and short residence times in the riser; thus, reducing the riser gas holdup. Downcomer gas holdup also decreased with increasing broth viscosity due to the tendency of large bubbles to disengage from the vessel.[7,8] The coalescence led to bimodal bubble size distribution as visually observed with the xanthan gum studies.[27] Larger bubbles reduced the rate of gas holdup increase due to a counteracting effect of the increase in bubble rise velocity.[7,28]

The experiments performed in this study demonstrated that the use of 1.94% CMC solution and a radial flow impeller worked better with the configuration of the airlift bioreactor, and the increase of viscosity (experiments performed with 1.80% xanthan gum) resulted in a dramatic reduction in gas holdup. The negative effect of the viscosity can be ascribed to the large drag forces promoting bubble coalescence in the distributor region, and the small bubbles stagnation against the wall of the reactor column, the aeration and agitation imposed were not strong enough to cause breakage of the bubbles and greater fluid circulation within the bioreactor. It is noteworthy that the increase in the rotation speed causes foaming and higher shear rates, which may impair the desired process performance.

The experimental data were correlated as a function of the mechanical power, the superficial gas velocity, and the kinematic viscosity, which were obtained from the following equations

$$\varepsilon_G = 0.30 \pm 0.04 \left(\frac{P_M}{V_L}\right)^{0.10\pm0.01} U_G^{0.88\pm0.03} \nu^{-0.01\pm0.01}, \text{(CMC)} \quad (12)$$

$$\varepsilon_G = 0.05 \pm 0.02 \left(\frac{P_M}{V_L}\right)^{0.06 \pm 0.02} U_G^{1.25 \pm 0.04} v^{-0.07 \pm 0.02}, \text{ (xanthan)} \quad (13)$$

Equations 12 and 13 describe that the gas holdup is mainly affected by the mechanical power as previously discussed; the imposed mechanical power depends on the agitation and the type of impeller used. The equation also demonstrates that even with the negative effect on the gas holdup, the viscosity affects the model.

Volumetric oxygen transfer coefficient

The volumetric oxygen transfer coefficient (k_La) was determined for the two types of fluids used in this study, at different rotation speeds and aeration curves; Figure 5 shows the curves obtained for each set of experiments.

The volumetric oxygen transfer coefficient dependence on the rotational speed revealed that the presence of agitation increased up to three times the k_La value, independent of the fluid type. However, the resulting values were relatively low, especially when xanthan gum was used as a fluid model.

Some authors reported a low oxygen solubilization capacity in viscous solutions using airlift bioreactors and bubble columns.[29,30] Our studies demonstrated that the increased viscosity decreases the k_La. The viscosity may increase with very little decrease in molecular diffusivity of oxygen in the aqueous phase.[10] The viscosity-increased effect on the volumetric oxygen transfer coefficient with the xanthan gum solutions using traditional airlift bioreactors has been studied extensively. Terasaka and Shibata[23] demonstrated that an increase in the viscosity drastically decreases the k_La; similar results were obtained in our studies when using 1.80% xanthan gum in the absence of agitation and at a same range of aeration. Conversely, comparative studies made by Cerri and Badino,[29] using three airlift bioreactors of different volumes and with the same similarities obtained higher k_La value with xanthan gum solutions than with glycerol solutions. These figures strongly disagree with the ones obtained by Terasaka and Shibata,[23] and also with our studies, in which the k_La did not exceed the value of 0.005 s^{-1}. Chisti and Jauregui-Haza[8] also achieved low k_La value for non-Newtonian fluid; however, when the airlift bioreactor was operated with agitation there was an increase of up to twice those obtained with traditional airlift. We observed that using the agitation in the bottom of the column and at the gas sparger outlet tripled the k_La, independently of the type of fluid.

The volumetric oxygen transfer coefficient depends not only on the properties of the fluid, but also on the superficial gas velocity, the bioreactor geometry, and agitation. Classical researches, such as the one conducted by Deckwer et al.,[31] in the bubble columns and using CMC viscous solutions, have shown that k_La is also a function of the type of gas sparger; they used perforated (73 holes of 1 mm diameter), sintered plate, and rubber plates. It was found that low gas velocities and rubber plates are more effective, according to these authors; there is a rapid increase in k_La value at the beginning of aeration up to the maximum point (homogeneous regime), followed by a small decrease (transition regime) until the k_La starts a slower linear rise (heterogeneous system), this trend was also observed with the sintered plate sparger. Although the perforated plate sparger presented lower values at a lower aeration velocity, it was observed that the k_La increase was almost linear, and only the homogeneous regime was observed. In our studies, we found that when using the perforated plate sparger (90 holes of 1 mm diameter) in the absence of agitation, the k_La values obtained with 1.94% CMC solution was very close to those obtained by Deckwer et al.,[31] at the same aeration interval. We also observed that when the bioreactor was operated with agitation there was a k_La increase, which follows a nearly linear trend. Some authors also reported the influence of reactor geometry on the k_La effect; according to Terasaka and Shibata,[23] there is significant k_La increase with the decrease in the diameter of the bioreactor column. Studies using xanthan gum solutions in stirred tank fermenter demonstrated the influence of both the impeller type and the number of blades in the volumetric oxygen transfer coefficient; the k_La value increases proportionally to the number of blades, with the paddle impeller showing the best results.[32] Previously, Herbst et al.,[33] had reached similar conclusions, when they observed a significant increase in the total power input, the k_La increase and the apparent viscosity decrease in stirred tank fermenter is directly correlated with the power input increase. According to these authors, the stronger viscosity effect at this low power input could be the result of poor mixing at high xanthan concentrations, which may limit oxygen transfer to a smaller part of the liquid volume. Our experiments (Figure 5) demonstrated that the correct choice of impeller could cause a significant k_La value increase in hybrid airlift bioreactors.

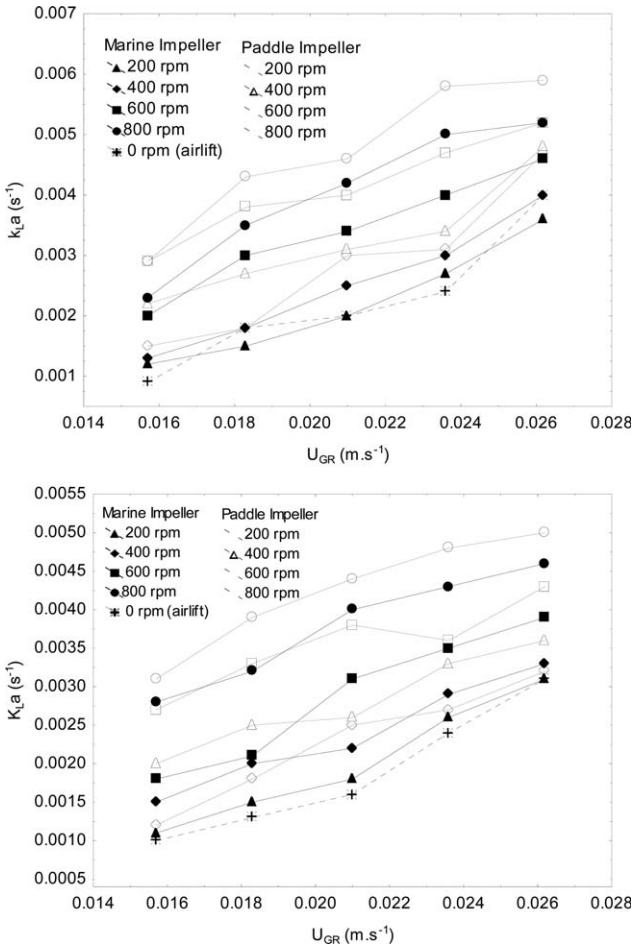

Figure 5. Effect of impeller agitation speed and the aeration velocity on the global oxygen mass-transfer coefficient for CMC 1.94% (a) and xanthan 1.80% (b).

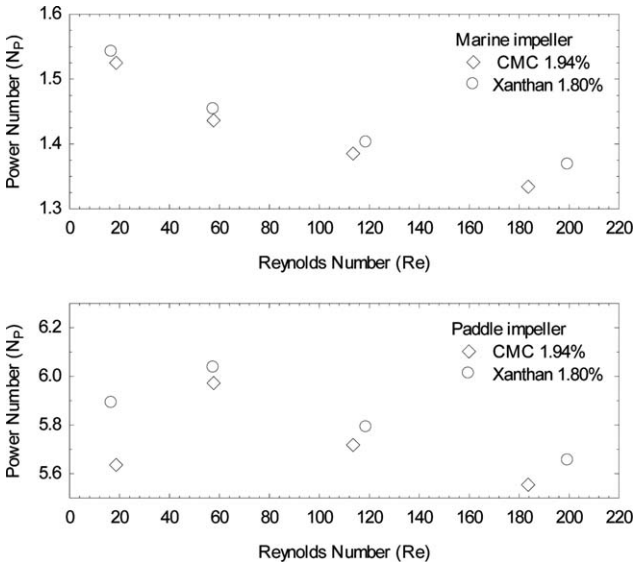

Figure 6. Variation of the measured power number with Reynolds number for the marine impeller and paddle impeller.

The k_La dependence on the superficial gas velocity was described as a function of superficial velocity U_G with the addition of mechanical power and apparent viscosity.

The empirical correlations were obtained using the experimental data (Figure 5) according to the equation described in Chisti and Jauregui-Haza[8]

$$k_La=0.02\pm0.01\left(\frac{P_M}{V_L}\right)^{0.10\pm0.04}U_G^{1.42\pm0.08}v^{-0.21\pm0.05},\ \text{(CMC)} \tag{14}$$

$$k_La=0.02\pm0.01\left(\frac{P_M}{V_L}\right)^{0.11\pm0.03}U_G^{0.99\pm0.04}v^{-0.08\pm0.03},\ \text{(xanthan)} \tag{15}$$

The correlations generated by the experimental data show that the effect of the increasing of U_G increases the k_La, while increasing of the viscosity decreases the k_La, as shown by the signals of the exponents.

Power measurement

Figure 6 presents the classic power curve in terms of the power number (N_P) vs. the Reynolds number (Re) for the two impellers and fluids used in our studies. The power number was defined by Eq. 7 and the Reynolds number by Eq. 9.

The experiments with non-Newtonian fluids and viscous (CMC 1.94% and 1.80% xanthan) resulted in low values of Reynolds number, characterizing the flow regime as transitional (Re ranged 20–200). In the studied limits, we could not verify the final of the laminar regime and the beginning of the transitional regime.

Figure 6 show that the power number presented significant changes with the Reynolds number. In general, the more viscous the higher the power number, this observation was confirmed in our experiments, where the solution of xanthan 1.80% had a slight increase in number of potency in relation to 1.94% of CMC solution. We also observed that the power number to the marine impeller showed lower values than the paddle impeller.

As a general rule, radial impellers have power values greater than axial impellers. The graphs presented in Figure 6 also show that there is no trend in the values obtained. Generally in the transitional flow region, there are large variations in power number, in contrast to the laminar flow zone where the power number decreases linearly with the increase of the Reynolds number or area corresponding to the turbulent regime, where the power number remains substantially constant with the increase of the Reynolds number. The results obtained for the marine impeller ranged from 1.33 to 1.54, while for the paddle impeller was between 5.55 and 6.04. Figure 7 illustrates the increase in power consumption with the increase in rotation speed imposed to the two impellers and fluids used in this study. The impeller power consumption in the case of aerated systems is always lower than that in unaerated systems as the transfer of power from the impeller to the fluid is greatly influenced by aeration. This power reduction is due to the formation of cavities behind the impeller blades and the different density of the fluid under gassed and ungassed conditions.[34] Figure 7 also shows that the difference between the energy imposed ungassed and gassed increases with rotation speed increasing. We observed that the power consumption was higher when the paddle impeller was used; this difference was approximately four times regarding the marine impeller. Energy consumption decreased by 25–40% when the bioreactor was aerated at different speeds of agitation and aeration. It has been shown that the gassed power input is usually 30–40% of the ungassed power input depending on the type of impeller and aeration rates used.[34]

Shear rate

The shear rate in mechanically agitated airlift bioreactors can be defined by the relative velocity between the bubbles and the liquid, and between the liquid and the walls from both the bioreactor and the impeller. The agitation caused by the impeller increases the shear rate, which varies according to the speed. The magnitude of variation depends on the specific location in the column, the type of impeller, agitation speed, and fluid properties. According to Al-Masry,[35] shear rates due to walls are significant and should not be neglected in the hydrodynamics of non-Newtonian systems. There remains considerable doubt as to the proper shear rate estimation for use in the design of airlift reactors. Although excess shear can result in loss of viability and cell disruption, a certain degree of shear rate is necessary to achieve sufficient mass transfer and energy.[36] The shear rate was calculated according to the methodology described by Sánchez Perez et al.,[37] modified for airlift bioreactors with stirring.

The average shear rate was calculated by adding the shear rate between the aerated part and the shear rate caused by agitation. According to Sánchez Perez et al.,[37] the shear rates for airlift bioreactors and non-Newtonian fluids following the power law are given by

$$\gamma_m=\left(\frac{1}{k}\frac{P_G}{V}\right)^{\frac{1}{n+1}} \tag{16}$$

where P_G is the power input due to aeration, and V is the volume.

For airlift bioreactor with mechanical stirring, the shear rate to non-Newtonian fluids that follows the power law will be given by the total specific power input that is the sum of power input due to gassing (P_G) and power input due to agitator (P_0).[8]

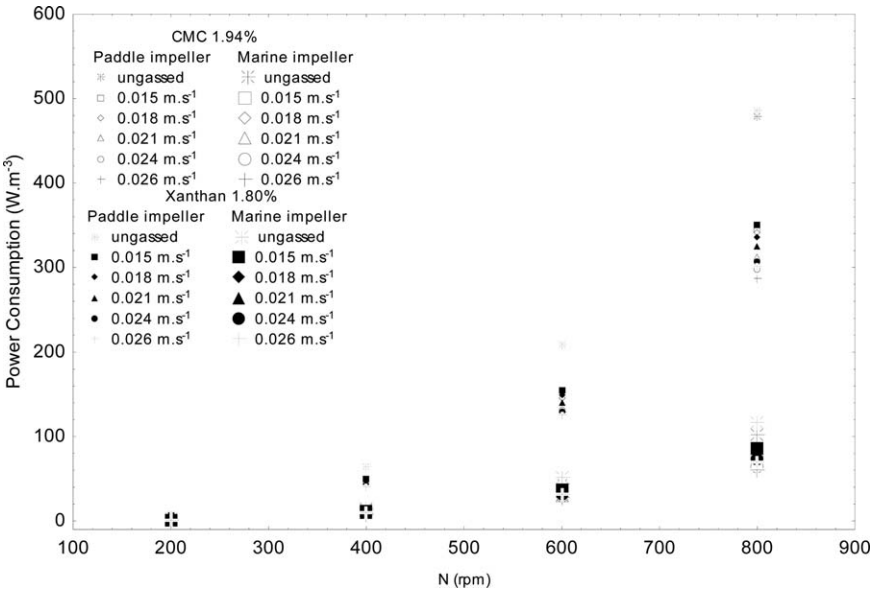

Figure 7. Ungassed and gassed power requirements of the marine impeller and paddle impeller over a range of agitation rates.

About the stirring system, we know that near the impeller, the velocity gradient is larger, and the apparent viscosity is diminished; thus, causing considerable turbulence in that area. As the liquid disperses from the impeller, the velocity decreases and the viscosity rises; however, the agitation is considered to be homogeneous and that there is an average strain rate for the system. Considering that the fluid moves around the agitator turbulently, and Figure 1 gives the geometry of the bioreactor, where $H_T = 10$ di; $d_T = 3$ di we have

$$\frac{P_0}{V} = \frac{2\pi NM}{\frac{45}{2}\pi \mathrm{di}^3} = \frac{4}{45\mathrm{di}^3} NM \tag{17}$$

In turbulent flow systems, the torque can be given by

$$M = \frac{N_p \rho_L \mathrm{di}^5}{2\pi} = N^2 \tag{18}$$

By applying (17) to (18), we have

$$\frac{P_0}{V} = \frac{N_p N^3 \mathrm{di}^5 \rho_L}{\frac{45}{2}\pi \mathrm{di}^3} \tag{19}$$

In stirred bioreactors, the energy is transmitted to the fluid mainly through the impellers, however, in hybrid airlift bioreactors, the total power input (P) is determined by the sum of the individual aeration contributions (P_G) and by the impeller (P_0), where the aeration power was calculated according to the following equation[8]

$$P_G = \rho_L g U_{GR} \tag{20}$$

For non-Newtonian fluids that follow the power law, we have

$$\gamma_m = \left(\frac{1}{k}\frac{P}{V}\right)^{\frac{1}{n+1}} \tag{21}$$

Figure 8 depicts the dependence of shear rate as a function of superficial gas velocity at different rotation speeds for the two types of impellers and fluids used. Figure 8 shows that the bulk shears rate increases with aeration and agitation speed. Higher shear rates are obtained when a radial impeller was used; however, at low rotational speeds (below 400 rpm), the shear caused by the radial impeller is very close to those obtained by the axial impeller or in the absence of agitation. The increases in shear, while using radial impellers, are probably caused by the increased turbulence; in these impellers, eddies form in the wake of the impeller blades and generate a high shear environment. The large liquid circulation in the column also increases the liquid contact with the wall of the bioreactor; thus, contributing to the increase in shear rate. Al-Masry[35] observed that, at low aeration rates, the ratio of wall shear rates to bulk shear rates is about 10% for xanthan and 32% for CMC.

Several methodologies have been proposed for calculating shear in bubble column and airlift reactors; however, there is a large disparity regarding these predictions.

Kawase and Kumagai[38] investigated the influence of rheological properties (k and n) and superficial gas velocity on the shear rate based on the concept of energy dissipation rate, and proposed a mathematical model for calculating the average shear rate in bubble column bioreactors given by

$$\gamma_m = (10.3\, n^{-0.63})^{1/(n+1)} (U_G g)^{1/(n+1)} (k/\rho_L)^{-1/(n-1)} \tag{22}$$

Other studies correlated to the shear rate average only as a function of superficial gas velocity. Shi et al.,[39] used CMC and xanthan gum solutions in an external loop airlift reactor. According to Shi et al.,[39] the measurement of local shear rate is complex because it is based on the fluid velocity profile throughout the bioreactor. According to these authors, the shear rate can be expressed by a quadratic equation given by

$$\gamma_m = 14800 U_G^2 - 351\, U_G + 3.26 \tag{23}$$

Grima et al.,[40] observed that the methodology used in Eq. 23 implied that shear rates were strictly wall shear rates, not bulk fluid shear rates. These observations were taken into account by Al-Masry[35] who studied the shear rate in CMC and xanthan gum solutions in an external loop airlift reactor; however, the average cross-sectional area ratio (A_d/A_r) was greater than the one found by Shi et al.,[39] who stated that the effective shear rate was not independent of the rheological parameters

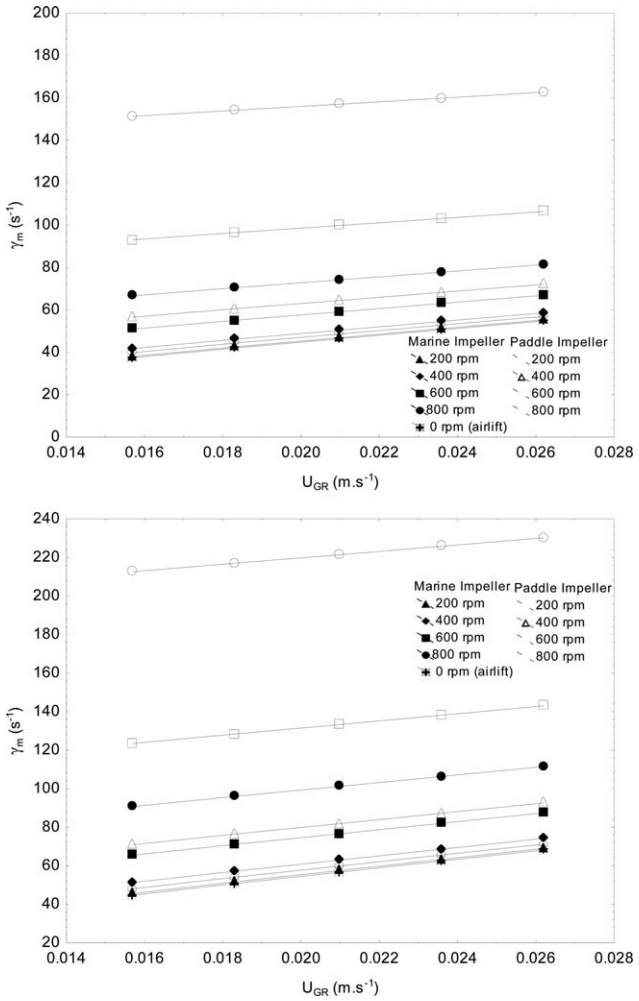

Figure 8. Effect of impeller agitation speed and the aeration velocity on the average shear rate for CMC 1.94% (a) and xanthan 1.80% (b).

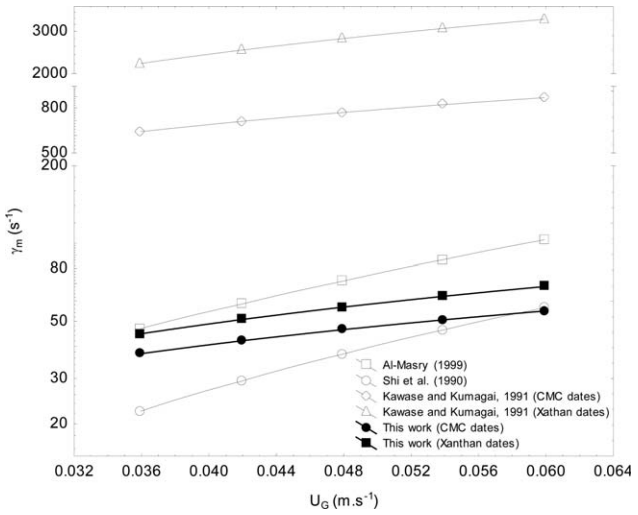

Figure 9. Comparison of average shear rate obtained in this work and through Eqs. 22–24.

of the solutions utilized in their study, and proposed two correlations, one for CMC and the other for xanthan gum. For a comparison with Shi et al.,[39] the estimated average shear rate plots are fitted to a second-order polynomial equation in a form similar to Eq. 23, and given by

$$\gamma_m = 24392 U_G^2 + 11.1 U_G + 14.9 \quad (24)$$

These models were only compared with the results obtained in this study when using an airlift bioreactor, as seen in Figure 9, that the models were significantly different from the model used in this study. However, it should be noted that the model used by Kawase and Kumagai[38] (Eq. 22) was developed for bubble columns. According to Al-Masry,[35] the power input in an airlift column is responsible not only for liquid flow in the riser, but for that in the downcomer as well, as is the case in a bubble column. Therefore, the Kawase and Kumagai model, as an approximation, is used for bulk average shear rates in airlift reactors. Similar studies made by Al Masry[35] also noted that shear rates in airlift reactors are lower than those encountered in bubble columns, which is particularly related to the fluid-defined flow path in airlift reactors. The model made by Shi et al.[39] showed lower shear rates compared to those obtained in this work. According to Chisti,[41] this model is not suitable for correlating mass transfer from gas bubbles or suspended solids because it does not give shear rates at gas-liquid or particle-liquid interfaces. The adjustment to the model from Al-Masry[35] showed similar results to the experimental data obtained with CMC solution; however, when compared to the results from xanthan gum, there is a significant difference, yet with the analysis of the curve tendency shown in Figure 9; this difference appears to decrease with intensification of the superficial gas velocity.

In our study, the methodology described by Sánchez Pérez et al.[37] and adapted to mechanically agitated airlift bioreactor showed results consistent with the results published in the literature for other types of reactors. It was found that the agitation increases the shearing, but the shear rate caused by the agitation is significant only when the bioreactor was operated with a rotation speed higher than 400 rpm, the volume below this shear rate remained close to that of a standard airlift bioreactor.

Bubble size

The average bubble size distribution has a great impact on mass transfer. Large bubbles present rapid ascent speed and low residence time in contrast with small bubbles that have a high residence time.

Both types of bubbles do not contribute much to the rate of mass transfer. Large bubbles have low residence time and small interfacial area and small bubbles deplete oxygen due to their small overall volume and large interfacial area.[18]

These two opposing mechanisms decide the degree of variation in mass transfer; however, they do not always show a direct correlation with the variation of gas holdup expected. With the increased viscosity, there is formation of a large boundary layer, increasing the resistance to mass transfer. Hence, only those turbulent eddies with sufficiently high energy can penetrate through this to cause bubble break-up or gas solute transfer, resulting in an overall decrease in mass-transfer coefficient which is more than that expected on the basis of the variation in the fractional gas phase holdup.[18,42]

Figure 10 illustrating the effect of viscosity on bubble size distribution at $U_{GR} = 0.0183$ m s^{-1} and Figure 11 shows the average distribution of bubbles in the bioreactor, where we can observe that the average size varied significantly with aeration. The experiments with viscous fluids showed that the

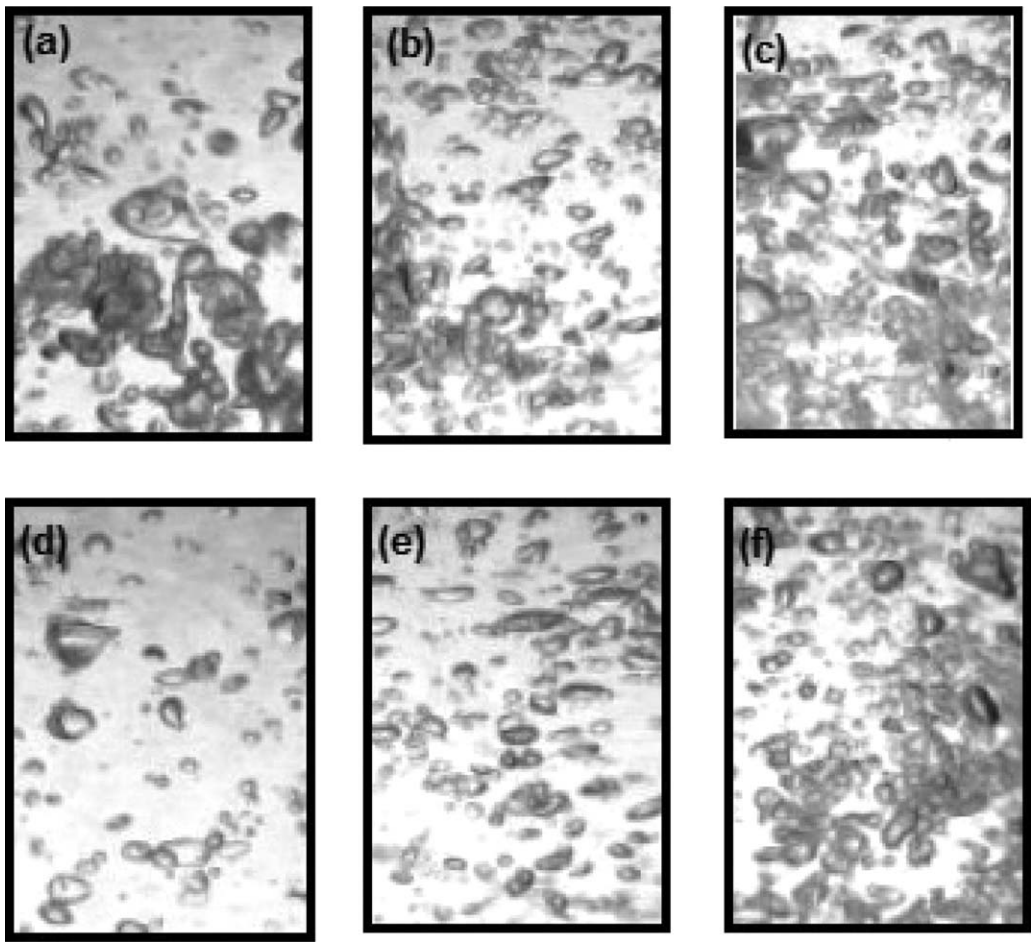

Figure 10. Images illustrating the effect of viscosity on bubble size distribution at $U_{GR} = 0.0183$ m s^{-1} for: (a) CMC 1.94%—airlift, (b) CMC 1.94% at 200 rpm, (c) CMC 1.94% at 600 rpm, (d) xanthan 1.80%—airlift, (e) xanthan 1.80% at 200 rpm, (f) xanthan 1.80% at 600 rpm.

presence of agitation helps to break up the bubbles. Studies in airlift bioreactor with xanthan gum and CMC have shown that the formation of small bubbles is caused mainly by the increased aeration. In our studies, the formed small bubbles multiplied with the increased aeration; these small bubbles were primarily formed in experiments with xanthan gum (Figure 11b). However, the presence of agitation had little influence on the smaller bubbles breakage when CMC was used as a fluid model (Figure 11a). In this case, the formation of coalescing bubbles was experimentally observed, especially when the bioreactor was operated with paddle impeller as mentioned above. The formation of coalescing bubbles was observed in the center of the bioreactor; the agitation did not cause a significant break up of these coalescing bubbles. In contrast, it was observed that the use of paddle impeller helped in the breaking up of the bubbles when xanthan gum was used as a fluid model (Figure 11b), the decrease in the diameter of the bubbles was higher when the bioreactor was operated with a higher agitation at 400 rpm. We observed that the viscosity and fluid characteristics might favor the formation of small bubbles, which can be reduced with the aid of agitation; however, these small bubbles stagnated in the bioreactor wall; the fluid high viscosity prevents their circulation on the bioreactor column. It is most likely that these stagnated small bubbles added a small contribution to the increase in the gas holdup and in the volumetric mass-transfer coefficient, with their contribution being greater with the increasing gas velocity. To explain the low k_La values (Figure 5), we decided to use the Calderbank[43] empirical correlation to determine the interfacial area, in this correlation the interfacial area (a) is a function of the gas holdup and the diameter of the bubbles, which was given by

$$a = \frac{6\varepsilon_G}{d_B(1-\varepsilon_G)} \tag{25}$$

Figure 12 shows the interfacial area calculated with Eq. 25, where the larger areas were obtained in the experiments performed with CMC and a paddle impeller. The interfacial area is caused mainly by the gas holdup, in which experiments with paddle impeller showed higher values (Figure 5). Figure 12 also shows that the CMC interfacial area was approximately five times that of the xanthan gum. According to Bhavaraju et al.,[44] the breaking of a bubble depends on the viscosity and the liquid-phase turbulence; the bubble size depends on the breakup at the sparger orifice and that the viscosity increase dramatically decreases the interfacial area; in pseudoplastic fluids, the apparent viscosity depends on the constants n and k of the employed model (Table 1).

However, the volumetric oxygen transfer coefficient (k_La) is directly dependent on the convective oxygen transfer coefficient (k_L) and its value being the product between the k_L and specific interfacial area (a).

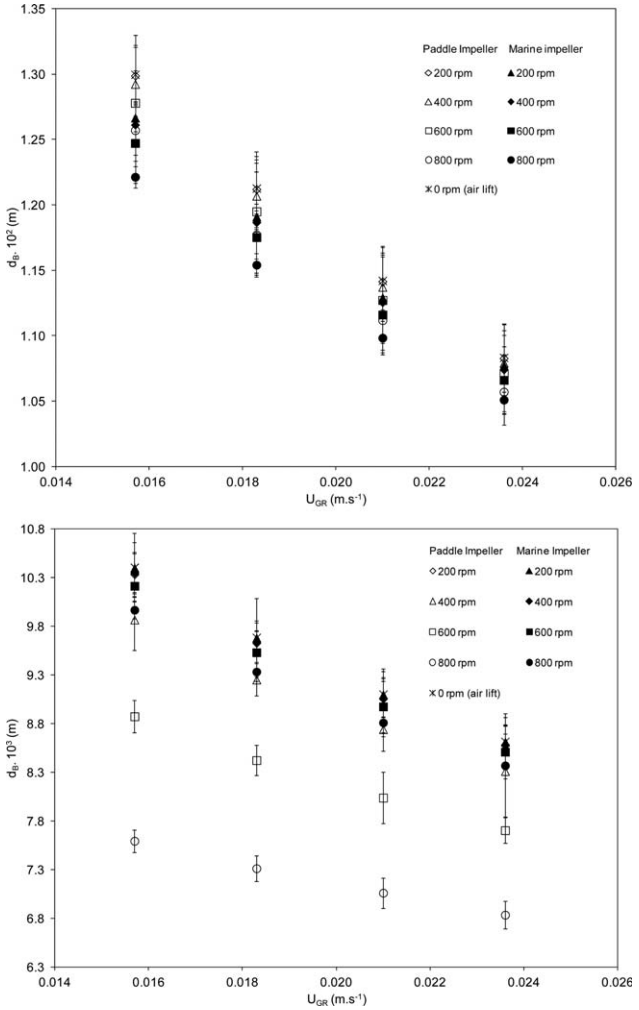

Figure 11. Effect of impeller agitation speed and the aeration velocity on mean bubble diameter for CMC 1.94% (a) and xanthan 1.80% (b).

The Ostwald–de Waele rheological model was used according to the equation proposed by Kawase et al.,[45] to predict convective oxygen transfer coefficient (k_L), this model is given by

$$k_L = C\sqrt{D_L}\left(\frac{\xi\rho_L}{k}\right)^{1/2(n+1)} \quad (26)$$

where D_L is the oxygen diffusion in liquid; ξ is the energy dissipation; C is the constant of proportionality, which according Kawase and Moo-Young[46] should be about 0.301.

Figure 13 depicts the dependence of the convective oxygen transfer coefficient as a function of the superficial gas velocity, calculated through Eq. 26. The graphs show that k_L remains practically constant for each condition of the study; whereas the higher values were obtained when using the paddle impeller. The model used in this study demonstrated that the use of a marine impeller results in very similar k_L values, independently of the type of fluid. It is also noteworthy that the use of a marine impeller in experiments with CMC resulted in k_L values lower than those obtained with the reactor operating in the traditional airlift mode. With the xanthan gum, the k_L values were very similar, except when the reactor was stirred with a paddle impeller with rotation speed of 800 rpm. These observations demonstrate that the increase in k_La values was caused

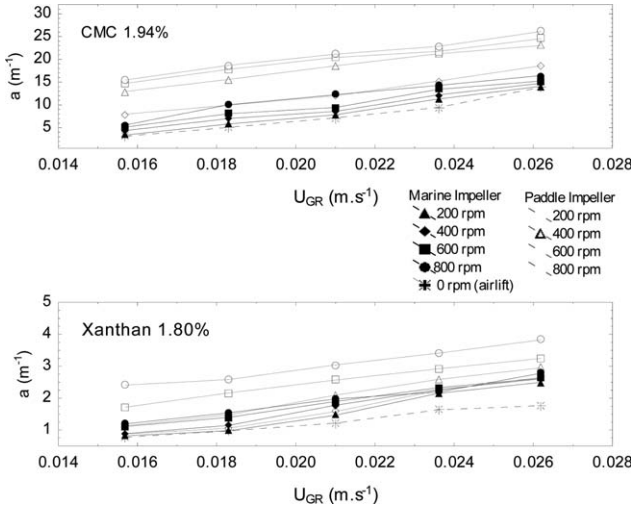

Figure 12. Interfacial area as a function of superficial gas velocity for CMC 1.94% (a) and xanthan 1.80% (b).

by the increased gas-liquid interfacial area and not by a convective oxygen transfer coefficient (k_L), that is, "a" is a direct function of the gas holdup (ε_G); thus, demonstrating that the k_La depends mainly on the gas holdup. Calderbank and Moo-Young[47] reported the influence of μ_{ap}, σ, and D_L on the k_L. Moreover, the k_L generally has a smaller increase when μ_{ap} increases or σ decreases. Kilonzo and Margaritis[10] also concluded that when the diffusivity decreases as a result of the viscosity increase, the k_L decreases more rapidly as the viscosity increases. In the volumetric mass-transfer coefficient, k_La also decreases as viscosity increases because the effective interfacial area (a) also decreases. Figure 13 shows that the convective oxygen transfer coefficient was higher when the reactor was operated with a solution of CMC and this value is 10 times greater than those obtained with the xanthan gum solution. To check the validity of Eqs. 25 and 26 on the experimental data, we calculated the theoretical k_La from the product (k_L) $\times$ (a). Figure 14 shows the quality of the adjustments within an error range of 20%.

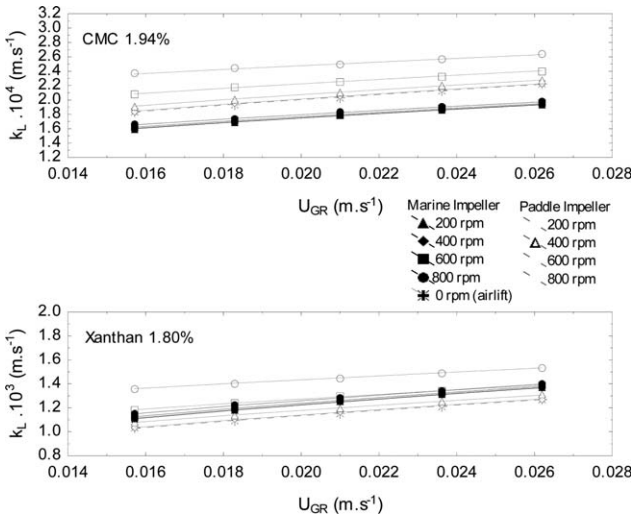

Figure 13. Convective oxygen transfer coefficient (k_L) as a function of superficial gas velocity for CMC 1.94% (a) and xanthan 1.80% (b).

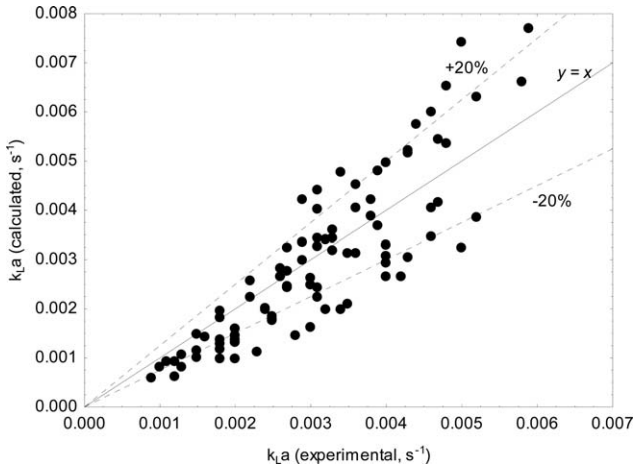

Figure 14. Comparison between the experimental and calculated data of the global oxygen mass-transfer coefficient.

Conclusions

In this article, we showed the influence of action of using an axial or radial impeller in hydrodynamic and in mass transfer of an airlift bioreactor with mechanical stirring when highly viscous fluids with rheological non-Newtonian behavior are used. Based on the results obtained in this study, we can conclude that the presence of agitation improves hydrodynamics and mass transfer.

The gas holdup and volumetric mass-transfer coefficient increased in up to five and three times, respectively, when compared to a conventional airlift bioreactor; however, better results were obtained when the straight paddle impeller type was used.

The increase in viscosity significantly reduces the mixing time, the gas holdup, and the mass transfer, which involves the shear rate increase. Although the best results stemmed from the use of a paddle impeller, we verified that a rotation velocity higher than 400 rpm causes a significant increase in the shear rate, which depending on the process used may be a limiting factor in the use of this bioreactor. The results suggest that the studied bioreactor can be used successfully in viscous fluid, and it can be more efficient than conventional airlift bioreactors. Therefore, based on these results we suggest the use of radial impellers.

Acknowledgment

The authors wish to acknowledge the financial support provided by the State of São Paulo Research Foundation (FAPESP, processes n° 2008/57873-8, 2010/04903-7 and 2010/03764-3).

Notation

a = gas-liquid interfacial area, m^{-1}
A_d = cross-sectional area of downcomer, m^2
A_r = cross-sectional area of riser, m^2
C = instantaneous concentration of dissolved oxygen, kmol m^{-3}
C_0 = initial concentration of dissolved oxygen, kmol m^{-3}
C^* = saturation concentration of dissolved oxygen, kmol m^{-3}
C_T = dimensionless tracer concentration defined by Eq. 3
d_B = mean bubble diameter, m
D_{DT} = diameter of draft-tube, m
D_T = tank diameter, m
D_L = diffusivity of the transferring gas in liquid, $m^2\ s^{-1}$
d_i = diameter of the impeller, m
E = fractional approach to equilibrium defined by Eq. 6
g = gravitational acceleration, $m\ s^{-2}$
H_A = column height, m
H_C = height between botton and draft-tube, m
H_{DT} = height of draft-tube, m
H_L = height of fluid, m
h = height between botton and impeller, m
h_D = height of gas-liquid dispersion, m
h_L = height of gas free liquid, m
k = consistency index, Pa s^n
k' = Herschel–Bulkley model coefficient, Pa $s^{n'}$
k_L = gas-liquid mass-transfer coefficient, $m\ s^{-1}$
k_La = overall volumetric gas-liquid mass-transfer coefficient, s^{-1}
m = stands for the size of the sample
M = torque, N m
M_0 = torque due to gearbox, bearings, and seals, N m
n = flow behavior index
n' = Herschel–Bulkley model index
N = rotational speed of the impeller, s^{-1}
N_p = impeller power number
P = total power input ($P_G + P_0$), W
P_G = power input due to gassing, W
P_M = power input due to agitator, W
Re = Reynolds number
s = standard deviation
t = time, s
t_0 = initial or start time, s
t_m = mean mixing time to achieve 95%, s
U_G = superficial gas velocity based on the total (riser + downcomer) cross-section, $m\ s^{-1}$
U_{GR} = superficial gas velocity in the riser zone, $m\ s^{-1}$
V = volume, m^3
V_L = volume of liquid, m^3
α = constant
γ_m = average shear rate, s^{-1}
ε = error
ε_G = overall fractional gas holdup
μ_{ap} = apparent viscosity according to the Ostwald–de Waele model, Pa s
μ = viscosity of liquid, Pa s
μ_G = gas viscosity, Pa s
v = kinematic viscosity, $m^2\ s^{-1}$
ρ_L = density of the liquid, kg m^{-3}
σ = interfacial tension, $N\ m^{-1}$
ξ = energy dissipation per unit mass, W kg^{-1}
τ = shear stress, Pa
τ_0 = yield stress, Pa

Literature Cited

1. Garcia-Ochoa F, Gomez E. Theoretical prediction of gas-liquid mass transfer coefficient, specific area and hold-up in sparged stirred tanks. *Chem Eng Sci*. 2004;59:2489–2501.
2. Albaek MO, Gernaey KV, Stocks SM. Gassed and ungassed power draw in a pilot scale 550 litre fermentor retrofitted with up-pumping hydrofoil B2 impellers in media of different viscosity and with very high power draw. *Chem Eng Sci*. 2008;63:5813–5820.
3. Xie M-h, Xia J-y, Zhou Z, Zhou G-Z, Chu J, Zhuang Y-P, Zhang S-l, Noorman H. Power consumption, local and average volumetric mass transfer coefficient in multiple-impeller stirred bioreactors for xanthan gum solutions. *Chem Eng Sci*. 2014;106:144–156.
4. Wei C, Wu B, Li G, Chen K, Jiang M, Ouyang P. Comparison of the hydrodynamics and mass transfer characteristics in internal-loop airlift bioreactors utilizing either a novel membrane-tube sparger or perforated plate sparger. *Bioprocess Biosyst Eng*. 2014;37:2289–2304.
5. Converti A, Zilli M, Arni S, di Felice R, del Borgh M. Estimation of viscosity of highly viscous fermentation media containing one or more solutes. *Biochem Eng J*. 1999;4:81–85.
6. Bang W, Nikov I, Delmas H, Bascoul A. Gas-liquid mass transfer in a new three-phase stirred airlift reactor. *J Chem Technol Biotechnol*. 1998;72:137–142.
7. Pollard DJ, Ison AP, Shamlou PA, Lilly MD. Reactor heterogeneity with *Saccharopolyspora erythraea* airlift fermentations. *Biotechnol Bioeng*. 1998;58:453–463.
8. Chisti Y, Jauregui-Haza UJ. Oxygen transfer and mixing in mechanically agitated airlift bioreactors. *Biochem Eng J*. 2002;10:143–153.

9. Espinosa-Solares T, de la Fuente EB, Tecante A, Medina-Torres L, Tanguy PA. Mixing time in rheologically evolving model fluids by hybrid dual mixing systems. *Trans IChemE*. 2002;80:817–823.
10. Kilonzo PM, Margaritis A. The effects of non-Newtonian fermentation broth viscosity and small bubble segregation on oxygen mass transfer in gas-lift bioreactors: a critical review. *Biochem Eng J*. 2004;17:27–40.
11. Pirouzi A, Nosrati M, Shojaosadati SA, Shakhesi A. Improvement of mixing time, mass transfer, and power consumption in a external loop airlift photobioreactor for microalgae cultures. *Biochem Eng J*. 2014;87:25–32.
12. Khare AS, Niranjan K. The effect of impeller design on gas hold-up in surfactant containing highly viscous non-Newtonian agitated liquids. *Chem Eng Process*. 2002;41:239–249.
13. Moucha T, Linek V, Prokopová E. Gas hold-up, mixing time and gas–liquid volumetric mass transfer coefficient of various multiple-impeller configurations: Rushton turbine, pitched blade and techmix impeller and their combinations. *Chem Eng Sci*. 2003;58:1839–1846.
14. Ju F, Cheng Z-M, Chen J-H, Chu X-H, Zhou Z-M, Yuan P-Q. A novel design for a gas-inducing impeller at the lowest critical speed. *Chem Eng Res Des*. 2009;87:1069–1074.
15. Chisti Y. *Airlift Bioreactors*. New York: Elsevier, 1989.
16. Camacho Rubio F, Sánchez Mirón A, Cerón García MC, García Camacho F, Molina Grima E, Chisti Y. Mixing in bubble columns: a new approach for characterizing dispersion coefficients. *Chem Eng Sci*. 2004;59:4369–4376.
17. Bandyopadhyay B, Humphrey AE, Taguchi H. Dynamic measurement of the volumetric oxygen transfer coefficient in fermentation systems. *Biotechnol Bioeng*. 1967;9:533–544.
18. Gogate PR, Beenackers AACM, Pandit AB. Multiple-impeller systems with a special emphasis on bioreactors: a critical review. *Biochem Eng J*. 2000;6:109–144.
19. Foucaut S, Ascanio G, Tanguy PA. Coaxial mixer hydrodynamics with Newtonian and non-Newtonian fluids. *Chem Eng Technol*. 2004;27:324–329.
20. Fadavi A, Chisti Y, Chriaštel L. Bubble size in a forced circulation loop reactor. *J Chem Technol Biotechnol*. 2008;83:105–108.
21. Godbole SP, Schumpe A, Shah YT, Carr NL. Hydrodynamics and mass transfer in non-Newtonian solutions in a bubble column. *AIChE J*. 1984;30:213–220.
22. Linek V, Sinkule J. Comments on validity of dynamic measuring methods of oxygen diffusion coefficients in fermentation media with polarographic oxygen electrodes. *Biotechnol Bioeng*. 1990;10:1034–1041.
23. Terasaka K, Shibata H. Oxygen transfer in viscous non-Newtonian liquids having yield stress in bubble columns. *Chem Eng Sci*. 2003;58:5331–5337.
24. Vasconcelos JMT, Alves SS, Barata JM. Mixing in gas-liquid contactors agitated by multiple turbines. *Chem Eng Sci*. 1995;50:2343–2354.
25. Nienow AW. On impeller circulation and mixing effectiveness in the turbulent flow regime. *Chem Eng Sci*. 1997;52:2557–2565.
26. Kawalec-Pietrenko BT. Time-dependent gas hold-up and bubble size distributions in a gas-highly viscous liquid-solid system. *Chem Eng J*. 1992;50:B29–B37.
27. Philip J, Proctor JM, Niranjan K, Davidson JF. Gas hold-up and liquid circulation in internal loop reactors containing highly viscous Newtonian and non-Newtonian liquids. *Chem Eng Sci*. 1990;45:651–664.
28. Mouza AA, Dalakoglou GK, Paras SV. Effect of liquid properties on the performance of bubble reactors with fine pore spargers. *Chem Eng Sci*. 2005;60:1465–1475.
29. Cerri MO, Badino AC. Oxygen transfer in three scales of concentric tube airlift bioreactors. *Biochem Eng J*. 2010;51:40–47.
30. Wen J, Jia X, Cheng X, Yang P. Characteristics of three-phase internal loop airlift bioreactors with complete gas recirculation for non-Newtonian fluids. *Bioprocess Biosyst Eng*. 2005;27:193–205.
31. Deckwer W-D, Nguyen-tien IC, Schumpe A, Serpemen Y. Oxygen mass transfer into aerated CMC-solutions in a bubble column. *Biotechnol Bioeng*. 1982;24:461–481.
32. García-Ochoa F, Gómez E. Mass transfer coefficient in stirrer tank reactors for xanthan solutions. *Biochem Eng J*. 1998;1:1–10.
33. Herbst H, Shumpe A, Deckwer W-D. Xanthan production in stirred tank fermenters: oxygen transfer and scale-up. *Chem Eng Technol*. 1992;15:425–434.
34. Gill NK, Appleton M, Baganz F, Lye GJ. Quantification of power consumption and oxygen transfer characteristics of a stirred miniature bioreactor for predictive fermentation scale-up. *Biotechnol Bioeng*. 2008;100:1144–1155.
35. Al-Masry WA. Effect of scale-up on average shear rates for aerated non-Newtonian liquids in external loop airlift reactors. *Biotechnol Bioeng*. 1999;62:494–498.
36. Contreras A, Garcıá F, Molina E, Merchuk JC. Influence of sparger on energy dissipation, shear rate, and mass transfer to sea water in a concentric-tube airlift bioreactor. *Enzyme Microb Technol*. 1999;25:820–830.
37. Sánchez Pérez JA, Rodríguez Porcel EM, Casas López JL, Fernández Sevilla JM, Chisti Y. Shear rate in stirred tank and bubble column bioreactors. *Chem Eng J*. 2006;124:1–5.
38. Kawase Y, Kumagai T. Apparent viscosity for non-Newtonian fermentation media in bioreactors. *Bioprocess Eng*. 1991;7:25–28.
39. Shi LK, Riba JP, Angelino H. Estimation of effective shear rate for aerated non Newtonian liquids in airlift bioreactors. *Chem Eng Commun*. 1989;89:25–35.
40. Grima EM, Chisti Y, Moo-Young M. Characterization of shear rates in airlift bioreactors for animal cell culture. *J Biotechnol*. 1997;54:195–210.
41. Chisti Y. Hydrodynamic damage to animal cells. *Crit Rev Biotechnol*. 2001;21:67–110.
42. Martín M, Montes FJ, Galán MA. Bubbling process in stirred tank reactors I: agitator effect on bubble size, formation and rising. *Chem Eng Sci*. 2008;63:3212–3222.
43. Calderbank PH. Physical rate processes in industrial fermentation, part 1: the interfacial area in gas-liquid contacting with mechanical agitation. *Chem Eng Res Des*. 1958;36:443–463.
44. Bhavaraju SM, Mashelkar RA, Blanch HW. Bubble motion and mass transfer in non-Newtonian fluids: part I single bubble in power law and Bingham fluids. *AIChE J*. 1978;24:1063–1070.
45. Kawase Y, Halard B, Moo-Young M. Theoretical prediction of volumetric mass transfer coefficients in bubble columns for Newtonian and non-Newtonian fluids. *Chem Eng Sci*. 1987;42:1609–1617.
46. Kawase Y, Moo-Young M. Mathematical models for design of bioreactors: applications of Kolmogoroff's theory of isotropic turbulence. *Chem Eng J*. 1990;43:B19–B41.
47. Calderbank PH, Moo-Young MB. The continuous phase heat and mass transfer properties of dispersions. *Chem Eng Sci*. 1961;16:39–54.

Manuscript received Sep. 21, 2014, and revision received Apr. 6, 2015.